Bond Dissociation Enthalpies of Large Aromatic Carbon-Centered Radicals

Karen Hemelsoet, Veronique Van Speybroeck,* and Michel Waroquier

Center for Molecular Modeling, Ghent University, Proeftuinstraat 86, 9000 Gent, Belgium

Received: February 21, 2008; Revised Manuscript Received: August 13, 2008

Carbon−hydrogen bond dissociation enthalpy (BDE) values are computed for the class of benzylic radicals. An extended and representative set of large methylated polyaromatics has been submitted to an accurate computational study using various levels of theory. The hybrid B3P86 as well as two contemporary functionals (BMK and M05-2X) are applied. For a selection of species, the suitability of the DFT methods is validated through comparison with high-level G3(MP2)-RAD and SCS-ROMP2 results. The influence of the polyaromatic environment on the BDE results is thoroughly discussed. The results are compared with other hydrocarbon radical types in order to obtain a generalized radical stability scale. In order to complete this investigation, also carbon−carbon BDE values have been calculated, giving information about the influence of the local environment on removing the methyl group from the polyaromatic.

1. Introduction

The bond dissociation enthalpy (BDE) is essentially a probe for the reaction enthalpy of the homolytic cleavage of the considered bond. The BDE is a good indicator of chemical reactivity since it represents a reliable measure of bond strength. There exist several compilations of experimental data on BDE values but these are mostly limited to small molecules.[1,2] Therefore, a lot of researchers have focused on the accurate theoretical calculation of BDEs. Focusing on carbon−hydrogen BDEs, we refer to refs 3−16. For a series of small hydrocarbon radicals including alkylic, allylic, and vinylic radicals and the propargyl, ethynyl, and phenyl radical, we recently published an extended set of C−H BDEs.[17] This essentially gave insight into the radical stability of a broad spectrum of carbon-centered radical species. For a lot of applications, however, larger polyaromatic radicals are of high interest. An important application field within petrochemistry concerns the steam cracking and parallel side process of coke formation.[18−20] The growth of a coke layer (which can be modeled as a network of conjugated six-membered rings) is examined by studying elementary reactions which involve various polycyclic aromatic hydrocarbons (PAHs) as model representatives. The knowledge of the thermodynamic characteristics of PAHs remains overall an ongoing challenge as they are not only key elements within incomplete combustion processes, but they also form the largest class of known carcinogens and mutagens.[21,22] In addition, they are present in substantial percentages in the atmosphere and in various celestial objects.[23,24] Previous work on arylic radicals showed that the polyaromatic environment can induce a maximum variation of about 20 kJ/mol (compared to the average value) on computed C−H BDEs.[17,19] The main factors inducing the variations are related to relief of steric hindrance in the parent molecule, whereas the stability of the product (σ-type) radicals is not substantially altered by the polyaromatic surroundings.[17]

It could be suspected that benzylic radicals which have a π-radical nature may be more sensitive to the local polyaromatic environment. To investigate this matter, the C−H BDEs of an extended set of methylated PAHs (as shown in Figure 1) in which bond breaking of a methyl hydrogen leads to the formation of benzylic radicals are calculated. It is generally known that, compared to the more easily formed benzylic radicals, arylic radicals are much more reactive for further reactions due to their less stable character. It is consequently clear that the activity dependence on the polyaromatic nature of both types could have important consequences for the formation of intermediates within polyaromatic growth.

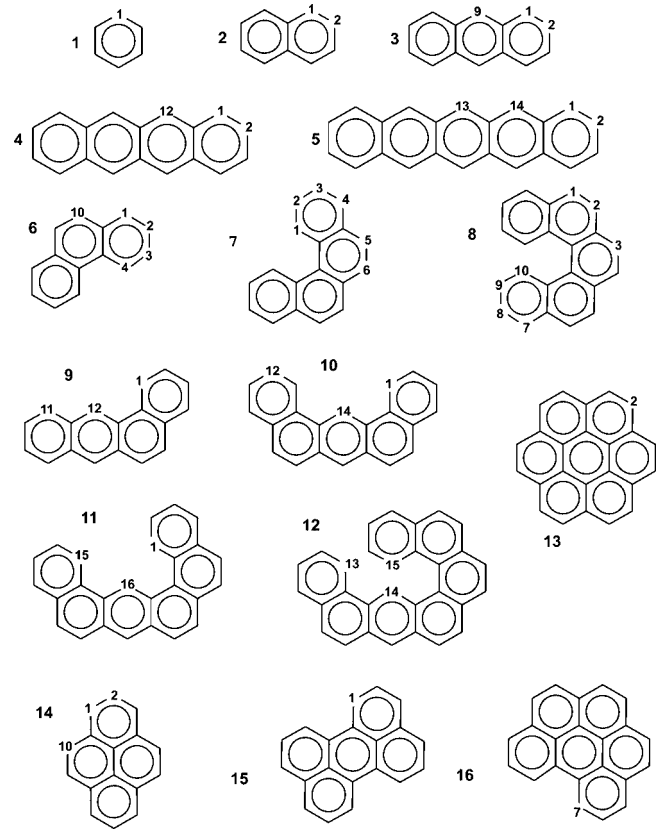

Figure 1. Selection of singly methylated PAHs. Methylation and subsequent abstraction can take place at different positions as indicated (the methyl group is not displayed in the figure).

* To whom correspondence should be addressed. Fax: 32 (0) 9 264 66 97. E-mail: Veronique.Vanspeybroeck@UGent.be.

10.1021/jp801551c CCC: $40.75
Published on Web 11/24/2008

Next to C−H BDEs, we also investigate the influence of the polyaromatic size and environment on carbon−carbon (C−C) BDEs for the methylated PAHs. Bond breaking of the attached methyl group leads to the set of arylic radicals. Papers in literature dealing with C−C BDE values of large aromatic compounds are very rare. Yao et al. computed C−C bond dissociation energies, bridging aromatic fragments using four DFT functionals (in particular, B3LYP, B3PW91, MPW1PW91, and B3P86).[25] The B3P86 functional was found to give the best agreement with available experimental data, showing an average deviation of 1.7 kcal/mol. Correlations between C−C bond lengths and corresponding BDE values have been investigated by Zavitsas,[26] testing 41 typical carbon−carbon bonds including single, double, triple, and highly strained bonds. He found an excellent linear relationship between both bond properties. A paper of Bauschlicher and Langhoff is of relevance with respect to this work as BDE values of methylated PAHs consisting of more than one aromatic ring have been calculated.[27] The authors conclude, on the basis of methylated naphthalene and anthracene, that the breaking of a methyl hydrogen to form a CH_2 side group is much easier than the loss of the entire methyl group or of an aromatic hydrogen.

The accurate calculation of BDEs has received a lot of attention in the last years. It has been shown that the reproduction of experimental BDEs within chemical accuracy, that is, showing a maximum deviation up to 4−8 kJ/mol, is not straightforward and demands the use of very expensive levels of theory such as post-Hartree−Fock or composite methods.[9,13,15] These methods are unfortunately often prohibitively time-consuming and therefore unfeasible for systems of large size. The development of new DFT functionals (generally characterized by an excellent cost-to-reliability performance) offers the possibility to compute BDEs in these cases. For the present work, it is, however, important to note that gradient-corrected DFT functionals are not properly constructed to handle strongly delocalized systems as they tend to overstabilize them. This fundamental shortcoming results in the failure to describe correctly the dissociation process. In addition, it leads to a systematic underestimation of barrier heights and BDEs of radical reactions. This issue was initially raised by Woodcock et al.[28] and further examined by Johnson et al.[7] Becke and co-workers have investigated this matter in detail and presented a real-space model of nondynamical correlation of post-HF style (resulting in the B05 functional) to deal with the aforementioned shortcomings of GGAs and hybrids.[29] In a very recent paper, the DF07 functional, unifying dynamical, nondynamical, and dispersion correlations, was proposed and tested for a variety of thermochemical and kinetic benchmark data, including bond dissociation enthalpies and barrier heights of radical reactions.[30] In this work, large π-type radicals are investigated, and therefore, we will investigate and discuss the GGA-related overstabilization issue. However, the calculation of relative BDEs (as is the focus in the present work) is not normally regarded as problematic. Nonetheless, recent work of Izgorodina et al.[11] indicates that various DFT methods, including several new generation functionals, can fail comprehensively to reproduce the correct qualitative trends in R−X BDEs with R = Me, Et, *i*-Pr, and *t*-Bu and X = H, CH_3, OCH_3, OH, and F. In our case, only one experimental value (i.e., for toluene) is available to benchmark the theoretical calculations. To validate whether qualitative trends are correctly predicted, we have performed G3(MP2)-RAD and SCS-ROMP2 calculations for a selection of our data set.

At present, the use of low-cost DFT functionals for the efficient computation of absolute and relative BDEs has been suggested by DiLabio et al. (B3P86),[3] Yao et al. (MPW1P86),[6] Senosiain et al. (KMLYP),[4] Izgorodina et al. (BMK),[11,13] and Zhao and Truhlar (M05-2X and M06-2X).[16] The aforementioned study of Izgororodina et al. in 2005[11] indicates that the best performance is offered by BMK, showing the smallest systematic errors in the relative BDEs. The MP2-based methods (i.e., SOS- and SCS-MP2) generally show larger errors (compared to those of the best DFT methods) for the absolute BDEs but better behavior for the relative BDEs. The same authors later on confirmed this conclusion,[13] putting forward the BMK functional as the best-performing DFT method, reproducing available experimental data on several radical addition, ring-opening, and hydrogen- and chlorine-transfer reactions with a similar accuracy as that of the composite G3(MP2)-RAD procedure. A very recent letter of Zhao and Truhlar[16] also investigates the performance of nine DFT functionals, using the same databases as those applied by Izgorodina et al. They concluded that the M06-2X and M05-2X functionals behave much better, as indicated by average mean deviations from benchmark values of 1.8 and 2.7 kcal/mol, respectively. Finally, we point out the very extended assessment of contemporary theoretical procedures performed by Menon et al.[15] BDE values, as well as radical stabilization energies (RSEs), were computed for a test set of 22 monosubstituted methyl radicals using a broad variety of up to 15 methods. This study included high-level results (e.g., W1 and G3(MP2)-RAD) as well as less-expensive DFT procedures (both restricted and unrestricted variations, in particular, B2-PLYP, MPW2-PLYP, BMK, MPWB1K, M05, and M05-2X). They concluded that the RMPWB1K and RBMK functionals are the best low-cost functionals to produce absolute BDE values, whereas their unrestricted counterparts systematically underestimate the benchmark W1 values by 6.3 and 4.5 kJ/mol, respectively. All DFT methods perform significantly better for the reproduction of relative BDEs (ΔBDEs).

As the present study also involves large methylated PAHs exhibiting a curled up geometry, the question arises whether dispersive (i.e., noncovalent) interactions are present. Modified DFT methods (called DFT-D) incorporating an empirical correction term (using damped interatomic potentials of the form C_6R^{-6}) have been suggested and tested in the literature.[31] These cost-effective methods provide, in addition to MP2-based methods, interesting alternatives for the very time-consuming methodologies based on coupled-cluster computations. In particular, Grimme and co-workers contributed to the recent progress made in this field, studying a variety of organic systems such as dimers, stacked graphene−nucleobase complexes, and so forth.[32] It is however not the scope of this work to perform an assessment of these DFT-D functionals for all studied PAHs. Nonetheless, results incorporating corrections from perturbation theory (describing part of the semilocal van der Waals correlation), in particular, B2PLYP and MP2-based values, will be presented.

It is clear that the search for new methodologies capable of adequately computing BDEs for large molecular systems is an ongoing effort.

2. Computational Details

All DFT calculations were performed using the Gaussian03 program.[33] The B3LYP functional,[34,35] in conjunction with the 6-31+G(d,p) basis set, was used to optimize geometries and to compute frequencies. This level of theory is known to provide a quantitatively good description of geometries, which has, in

TABLE 1: C−H BDEs (in kJ/mol) of the Investigated Linear Methylated Polyaromatics[a]

X	B3P86	BMK	M05-2X	ROMP2 (1)	SCS-ROMP2 (1)	ROMP2 (2)	SCS-ROMP2 (2)	G3(MP2)-RAD
1-1	376.1	372.8	370.4	354.3	371.1	372.0	392.7	374.1
2-1	371.4	368.5	368.2	354.0	374.3	369.3	393.6	370.2
2-2	373.1	370.0	367.5	352.5	370.7	369.2	391.4	371.4
3-9	350.7	345.8	344.4	333.7	353.0	350.0	371.2	350.9
3-1	365.8	363.4	361.6	339.2	367.7	353.2	384.0	363.5
3-2	366.4	363.9	361.4	337.7	365.4	354.6	383.7	364.4
4-12	335.1	328.1	323.0					
4-1	361.4	359.2	356.0					
4-2	359.6	357.4	354.8					
5-13	311.6	301.3	295.3					
5-14	323.6	315.1	308.7					
5-1	357.4	355.6	351.2					
5-2	353.5	351.6	345.2					

[a] Values are calculated using B3LYP/6-31+G(d,p) geometries and B3P86/6-311G(d,p), BMK/6-311+G(3df,2p), or M05-2X/6-311+G(3df,2p) scf energies. ROMP2 scf energies, with a small (1: 6-31G(d)) and large (2: 6-311+G(3df,2p) for **1** and **2** and 6-311G(d,p) for **3**) basis set are given. G3(MP2)-RAD results are also included. The structure labels are depicted in Figure 1.

particular, been shown for radical hydrogen abstractions at PAHs in refs 36 and 37. The choice of the level of theory for the subsequent single-point energy calculations was based on various grounds. First of all, the scf computations were performed using B3P86/6-311G(d,p) in order to allow comparison with earlier BDE values computed in ref 17. Second, the literature review taken up in the Introduction promotes the use of the hybrid-meta BMK functional,[38] in combination with the 6-311+G(3df,2p) basis set. The latter functional is generally known to reproduce reaction barriers within an accuracy of approximately 10 kJ/mol[38] and has shown promising results in previous works on radical reactions.[37,39] Finally, the recently developed M05-2X functional (available in the latest version E.01 of Gaussian03) was also chosen for the single-point energy calculations (combined with a 6-311+G(3df,2p) basis set). This functional also belongs to the hybrid-meta class of DFT methods and is a high-nonlocality functional with double the amount of nonlocal exchange (compared to that of the M05 method). It is parametrized only for nonmetals.[40] All DFT computations involving the open-shell radical species were performed using the unrestricted methodology.

Additional calculations at a high level of theory were performed on a selection of PAHs. First of all, ROMP2 single-point energies and the spin-modified versions SCS-ROMP2[41] and SOS-ROMP2[42] (in combination with the 6-31G(d), 6-311G(d,p), or 6-311+G(3df,2p) basis set and B3LYP geometries) were applied for the smallest representatives of the model PAHs. High-level G3(MP2)-RAD C−H BDEs are reported for toluene, methylated naphthalene, and methylated anthracene.[43] These types of calculations fall for the larger species beyond our computational resources. Moreover, the structures for which the various DFT functionals show large discrepancies are submitted to B2PLYP/6-311+G(3df,2p) and ROMP2/6-31G(d) single-point energies using the B3LYP geometries. The MP2 and URCCSD(T) (part of the G3(MP2)-RAD method) computations were performed using the MolPro software package.[44] The B2PLYP functional, as proposed by Grimme, is a new hybrid DFT functional containing a large amount of exact exchange (i.e., 53%) as well as a perturbative second-order correlation part (27%).[45] However, due to the computation of the MP2 correlation energy, the unrestricted B2PLYP results are hampered by the well-known problem of spin contamination.

Both the G3(MP2)-RAD results and those including second-order perturbation theory allow us to address the issue of overstabilization of delocalized radicals with traditional DFT functionals as well as the question whether it is necessary to include dispersion effects. The former is mainly a problem when dealing with the series of linear methylated PAHs (vide supra), whereas the latter mostly concerns the nonlinear species which exhibit curled up geometries.

3. Results and Discussion

A comprehensive test set of singly methylated PAHs is examined. Methylation can take place at different positions at the PAH; all investigated physically distinguishable sites are indicated in Figure 1. The numbering conforms to the IUPAC convention. Two subcategories can be distinguished, a linear (species **1**−**5**) and a nonlinear series (species **6**−**16**).

3.1. Computational Accuracy. *C−H BDEs.* The obtained carbon−hydrogen BDE values are defined as

$$\mathrm{BDE(R{-}H)} = [\Delta_f H_{298}(\mathrm{R}) + \Delta_f H_{298}(\mathrm{H})] - \Delta_f H_{298}(\mathrm{R{-}H}) \quad (1)$$

with $\Delta_f H_{298}$(R) and $\Delta_f H_{298}$(R−H) as the enthalpies of formation of the radical benzylic species (R) and the molecule (R−H), respectively. The computed BDEs are given in Tables 1 and 2 for the series of linear and nonlinear polyaromatics, respectively. Results are reported using the three chosen functionals B3P86, BMK, and M05-2X. It is seen that the values are, in general, slightly shifted with respect to each other; however, all qualitative trends are maintained. The B3P86 and M05-2X predictions correspond to the maximal and minimal BDEs, with average values of 365.0 and 359.3 kJ/mol, respectively. The BMK values are found to lie between these two extremes, with an average value of 361.7 kJ/mol. All three methods predict BDEs which can vary largely in terms of the polyaromatic environment (up to 75 kJ/mol). This confirms our anticipation that benzylic radicals are much more prone to variations of BDEs than arylic radicals.

Overall, the results using the three methods are for the majority of the investigated species reasonably close to each other; however, discrepancies up to 16 kJ/mol (for **5-13**) are obtained. In order to get a better view on which method is preferable and to ensure that the correct qualitative trends are obtained, the following steps are undertaken. First of all, computed results are compared with experimental data. Unfortunately, there are only results available for the C−H BDE of toluene. Therefore, our values are also compared with other theoretical results reported in the literature. In a next step, the C−H BDEs of the species **1**, **2**, and **3** are computed using more

TABLE 2: C−H BDEs (in kJ/mol) of the Investigated Nonlinear Methylated Polyaromatics[a]

X	B3P86	BMK	M05-2X	X	B3P86	BMK	M05-2X	X	B3P86	BMK	M05-2X
6-4	370.7	368.7	365.5	**8-9**	372.2	369.7	366.9	**11-1**	368.9	366.0	363.7
6-3	372.7	370.0	366.1	**8-8**	373.0	370.2	367.5	**11-16**	346.7	341.5	339.8
6-2	374.5	371.6	367.8	**8-7**	372.7	369.9	368.0	**11-15**	377.3	374.9	371.7
6-1	374.4	371.8	370.5	**8-1**	370.1	367.4	365.6	**12-13**	382.0	371.9	371.2
6-10	373.1	370.0	368.9	**8-2**	373.6	370.7	368.3	**12-14**	346.2	342.4	341.1
7-1	367.3	365.1	362.9	**8-3**	372.2	369.8	368.1	**12-15**	371.1	367.2	365.1
7-2	371.7	369.0	366.5	**9-1**	371.7	369.9	366.9	**13-2**	377.2	371.6	370.5
7-3	373.5	370.8	368.2	**9-12**	351.6	348.4	346.5	**14-1**	364.2	361.6	359.9
7-4	372.8	370.3	368.6	**9-11**	366.7	364.4	362.5	**14-2**	377.9	374.2	372.0
7-5	371.4	369.0	366.9	**10-14**	344.6	342.4	341.3	**14-10**	372.0	368.7	367.2
7-6	374.1	371.2	369.1	**10-1**	370.6	369.1	366.7	**15-1**	353.1	351.5	349.6
8-10	366.8	367.7	365.4	**10-12**	376.9	373.7	375.3	**16-7**	364.0	358.6	357.2

[a] Values are calculated using B3LYP/6-31+G(d,p) geometries and B3P86/6-311G(d,p), BMK/6-311+G(3df,2p), or M05-2X/6-311+G(3df,2p) scf energies. The structure labels are depicted in Figure 1.

sophisticated levels of theory, that is, the G3(MP2)-RAD and standard and modified ROMP2 methods. In a final step, single-point energies are computed for structures **5** and **10** using the B2PLYP functional and ROMP2-based methods. The latter step allows one to assess the performance of the three tested DFT functionals with respect to the overstabilization issue as well as to the inclusion of dispersion effect (as mentioned earlier).

First, the assessment is made with respect to toluene (**1**-**1**). Various experimental values of the C−H BDE of toluene can be found in the literature. Tsang reports a value of 375.0 ± 8.4 kJ/mol,[46] Berkowitz et al. report 370.3 ± 6.3 kJ/mol,[47] and Blanksby and Ellison report 375.3 kJ/mol.[2] A comparison of our results with the latter (most recent) experimental BDE estimate indicates a minor deviation of 0.8 kJ/mol for the B3P86 functional. Also, BMK performs quite well, with a slight underestimation of −2.5 kJ/mol. The M05-2X functional shows the largest, but still acceptable, deviation (−4.9 kJ/mol).

The C−H BDE value of toluene has also been the subject of various theoretical studies. Comparison between all data should occur carefully as there is no consistency in reporting bond dissociation properties (e.g., inclusion of ZPVEs and/or thermal corrections to the enthalpy, at 0 or 298 K, etc.). We will systematically report BDEs at 298 K following the definition of eq 1 unless otherwise specified. BDEs for the benzylic C−H bond were calculated for the first time in 1996 by Fox and Kollman[48] using BLYP and B3LYP (current functionals at that time) as well as HF and MP2. The best performance was offered by B3LYP (394.9 kJ/mol) for toluene. In 2003, Yao et al. reported B3P86 and MPW1P86 results in close agreement with experiment.[6] In addition, Nam et al. have also provided BDE values of toluene and their substituted derivatives using three hybrid DFT functionals (B3PW91, B3LYP, and O3LYP).[10] In particular, the RO version of the latter two functionals performs well. More advanced DFT methods have been assessed by Izgorodina et al.,[13] Zhao et al.,[16] and Menon et al.[15] In particular, we mention the values of 369.5 and 373.2 kJ/mol for the benzylic C−H BDEs in toluene at 0 K using the high-level G3(MP2)-RAD and W1 methods, respectively.[15] Our BDE results at 0 K using the three levels B3P86, BMK, and M05-2X amount to 371.4, 368.2, and 365.8 kJ/mol, respectively (shift of about 4.7 kJ/mol with respect to enthalpies at 298 K; see Table 1). Taking the W1 result as a benchmark, the moderate deviations of 1.8, 5.0, and 7.4 kJ/mol are obtained for the corresponding levels. Comparing our values to both experimental and other high-level results shows that all three DFT functionals perform more than reasonable. However, this single good agreement is not a guarantee that correct chemical trends will be predicted for a larger set of species (as reported earlier in the literature).[11] Therefore, further validation of our results is needed.

For a selection of methylated PAHs, the DFT results are compared with more sophisticated computational data. G3(MP2)-RAD values were calculated for toluene, methylated naphthalene, and methylated anthracene; the results can also be found in Table 1. These were the only possible molecules within the current computational resources as, due to the URCCSD(T) single-point energy computations, this method becomes rapidly unfeasible for larger systems. As the SCS-ROMP2 and SOS-ROMP2 behave in a similar way, the latter results are not explicitly tabulated here. First of all, we again compare with the experimental BDE value of toluene (375.3 kJ/mol). The SCS-ROMP2 with a small basis set and the ROMP2 with the large basis set give good agreement. As expected, our "best theoretical" method, that is, G3(MP2)-RAD, reproduces the experimental value almost exactly. G3(MP2)-RAD predicts the BDE of **2**-**1** (i.e., a naphthalene-like site) slightly lower than that of **2**-**2** (i.e., a benzene-like site). This trend is not reproduced by the various MP2-based methods, whereas B3P86 and BMK do give the correct qualitative trend. In view of the small energy differences, definite conclusions can only be made when trends for a larger set are examined. The results for methylated anthracene (**3**) are also shown, indicating C−H BDEs which strongly depend on the methylation site. There is an excellent agreement between the B3P86 and BMK results and the benchmark G3(MP2)-RAD data. The qualitative trend (i.e., the ΔBDE between **3**-**9** and **3**-**1** or **3**-**2** being very large, whereas the BDEs of **3**-**1** and **3**-**2** are very similar) is maintained in every case, despite the sometimes large discrepancies in absolute values. The standard ROMP2 ΔBDE results (with a small and large basis set) are too small compared with the reference data; therefore, this method is not recommended for the study of relative BDE values. Moreover, Table 1 shows that the combination of the standard ROMP2 method with the small basis set results in absolute BDE values which are clearly too low. It is however very encouraging to see that the results are substantially shifted upward (on average, by 16 kJ/mol) when applying the spin-modified variants SCS- and SOS-ROMP2. On the basis of previous analysis, the SCS-ROMP2/6-31G(d) will be used for further validation of the low-cost DFT results.

In a final step to investigate the appropriateness of various methods for the computation of C−H BDEs, we examine, in more detail, structures **5** and **10**, a representative linear and nonlinear PAH, for which the aforementioned DFT results show in particular for site **5**-**13** large discrepancies. The results are

TABLE 3: C−H BDEs (in kJ/mol) of Species 5 and 10[a]

X	ROMP2	SCS-ROMP2	SOS-ROMP2	B2PLYP
5-13	287.2	304.7	301.7	332.6
5-14	301.2	319.6	316.5	351.0
5-1	336.7	362.6	358.3	356.6
5-2	338.5	361.7	356.6	352.7
10-14	315.1	335.7	331.9	352.9
10-1	348.2	367.6	366.6	369.9
10-12	354.5	371.7	370.1	370.9

[a] Values calculated using B3LYP/6-31+G(d,p) geometries and ROMP2/6-31G(d) or B2PLYP/6-311+G(3df,2p) scf energies. The structure labels are depicted in Figure 1.

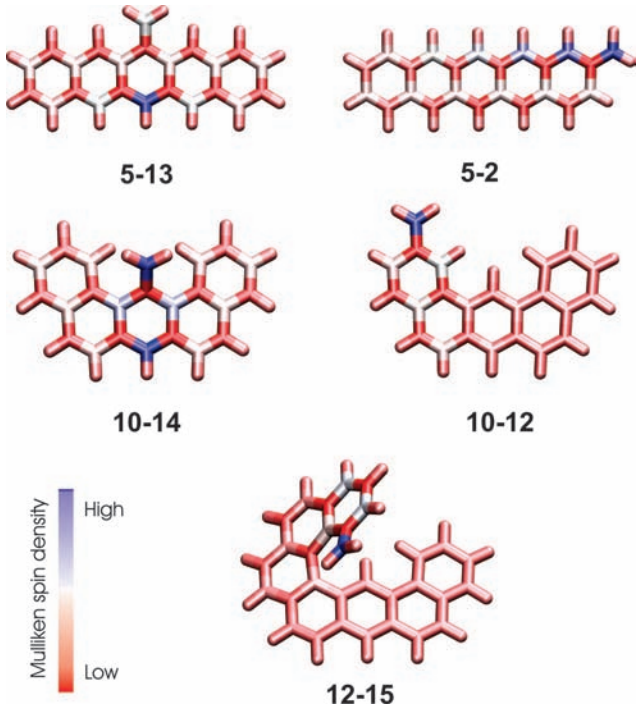

Figure 2. Mulliken atomic spin densities for the benzylic radicals **5-13**, **5-2**, **10-14**, **10-12**, and **12-15** (see Figure 1).

tabulated in Table 3. The trend in SCS-ROMP2/6-31G(d) energies for both molecules corresponds to the trend predicted by the three tested DFT functionals, although relative differences between BDEs at various sites might differ, for example, the ΔBDE between **5-13** and **5-2** varies from 41.9 (B3P86) to 54.9 (SOS-ROMP2/6-31G(d)). For B2PLYP, the trend deviates, but these values are hampered by strong spin contamination. As far as the absolute BDE values can be compared, it is seen that the M05-2X predictions are too low. Overall, the BMK results are in closest agreement with the reference SCS-ROMP2 values. Structure **5** is the largest linear PAH of our data set and exhibits strong delocalization of the unpaired electron. This can be seen in Figure 2, where the spin density is plotted for various molecules. In the figure, the spin polarization for the strongly delocalized molecules **5-13** and **5-2** is clearly visualized. It is also illustrated that deviations from planarity result in the decrease of the delocalization effect, for example, for structures **10-12** and **12-15**, which exhibit a curled up geometry. Comparison of the SCS-ROMP2 and DFT results for the C−H BDEs of the nonplanar structures **10-1** and **10-12** also indicates that dispersion contributions (not present in DFT) have no significant influence. Previous discussion shows that the examined DFT methods provide valuable and cost-effective levels of theory for the accurate computation of C−H BDEs of large methylated PAHs.

TABLE 4: C−C BDEs (in kJ/mol) of the Investigated Methylated Polyaromatics[a]

X		X		X		X	
1-1	429.3	**6-4**	394.7	**8-8**	431.9	**11-15**	396.8
2-1	429.6	**6-3**	430.8	**8-7**	426.6	**12-13**	398.9
2-2	431.0	**6-2**	432.1	**8-1**	430.3	**12-14**	356.3
3-9	418.7	**6-1**	427.3	**8-2**	427.2	**12-15**	393.7
3-1	430.6	**6-10**	428.8	**8-3**	428.6	**13-2**	431.3
3-2	432.4	**7-1**	375.3	**9-1**	395.5	**14-1**	430.3
4-12	417.2	**7-2**	429.8	**9-12**	386.7	**14-2**	429.5
4-1	433.4	**7-3**	432.4	**9-11**	428.1	**14-1**	430.9
4-2	432.3	**7-4**	426.7	**10-14**	353.8	**15-1**	398.5
5-13	419.2	**7-5**	430.1	**10-1**	394.5	**16-7**	395.3
5-14	420.3	**7-6**	427.5	**10-12**	435.1		
5-1	431.0	**8-10**	395.6	**11-1**	376.1		
5-2	432.2	**8-9**	429.7	**11-16**	341.7		

[a] Values are calculated at the BMK/6-311+G(3df,2p)//B3LYP/6-31+G(d,p) level of theory. The structure labels are depicted in Figure 1.

C−C BDEs. We have also computed (for the same set of methylated PAHs) C−C BDE values defined as

$$\mathrm{BDE(R'-CH_3)} = [\Delta_f H_{298}(\mathrm{R'}) + \Delta_f H_{298}(\mathrm{CH_3})] - \Delta_f H_{298}(\mathrm{R'-CH_3}) \quad (2)$$

with R′ representing arylic radicals.

The obtained results, calculated at the BMK/6-311+G(3df,2p)//B3LYP/6-31+G(d,p) level of theory, are given in Table 4. A comparison of the C−C BDE value of toluene with available experimental data confirms the accuracy of the suggested level of theory, as the most recent experimental value amounts to 433.0 kJ/mol (deviation of −3.7 kJ/mol).[2] Older experiments were performed by McMillen and Golden[49] and Lias et al.[50] The aforementioned study of Yao et al.,[6] examining five hybrid DFT functionals, reported on the good performance of B3P86, MPW1P86, and ROB3P86. We also point out that our results for the smallest methylated molecules **1**, **2**, and **3** correspond in a reasonable way with those obtained by Bauschlicher and Langhoff.[27]

3.2. Reactivity Scale of Carbon-Centered Radicals. The computed benzylic C−H BDE results (see Tables 1 and 2) are plotted on the BDE scale including different types of radicals. The B3P86//B3LYP results are used to allow comparison with earlier results of ref 17. Corresponding to experimental findings, the following sequence was obtained: ethynylic, arylic, vinylic, alkylic, benzylic, propargylic, and allylic given in order of increasing stability and displayed in Figure 3. In the present work, the series of arylic and, in particular, benzylic radicals have been substantially increased compared to ref 17. Both families have an essentially different stability pattern. The arylic radicals are characterized by relatively large C−H BDE values, indicating a rather unstable nature, which essentially can be related to its σ-type character. The benzylic radicals have C−H BDEs which are, on average, 100 kJ/mol lower as they are characterized by an enhanced resonance stability.[51,52]

3.3. Influence of the Polyaromatic Environment on C−H BDEs. In the remainder of this article, we will use the BMK//B3LYP results in order to allow a consistent analysis. All C−H BDE values are visualized on an enlarged scale in Figure 4. The influence of a polyaromatic environment within each radical family is found to be significantly different. For the series of arylic radicals, various computational studies have suggested a segregation of the BDEs into six distinct subclasses, depending on the specific site from which a hydrogen is abstracted.[17,53−57]

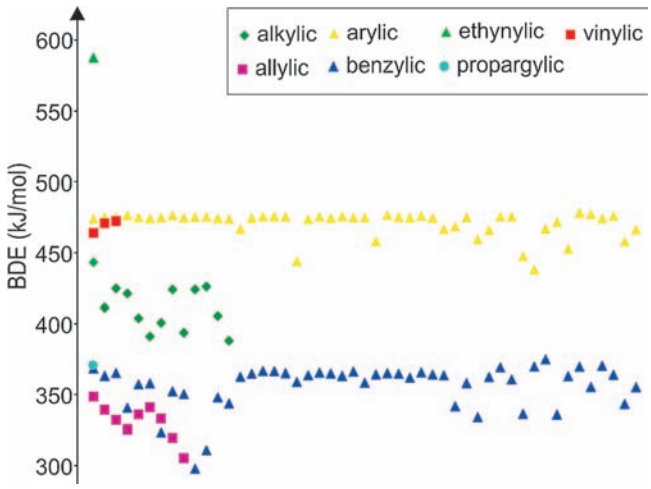

Figure 3. C−H BDEs (in kJ/mol) of various radical types, calculated at the B3P86/6-311G(d,p)//B3LYP level of theory. The set of arylic and, in particular, benzylic radicals have been substantially increased compared to ref 17.

It was found that the size of the model molecule has a minor influence on the BDE values. The C−H BDEs are more or less concentrated around an average value of 465.4 kJ/mol, with a maximum spread of 33.3 kJ/mol. The question arises if similar conclusions also hold for C−H BDEs on methylated PAHs, leading to benzylic radicals. First of all, a segregation into distinct categories does not appear for the whole test set. The majority of the C−H BDE predictions in methylated polyaromatics range between 360 and 380 kJ/mol, with an average value of 361.7 kJ/mol. The largest deviations are noticed for the subcategory of linear methylated PAHs. The variations can rise to 71 kJ/mol. The extremes are given by methylated pentacene (**5**-**13**) (301.3 kJ/mol) and toluene (**1**-**1**) (372.8 kJ/mol). Two distinct features are manifest. First, the size of the linear methylated structure plays a significant role; the longer the chain, the smaller the C−H BDE value. This observation is in correspondence with an enhanced delocalization of the unpaired electron in the larger product radicals and could be anticipated from the π-character of the radical. A second feature concerns the BDE dependence on the site (or position) where the methylation has occurred. This can be explicitly shown for the structures **3**, **4**, and **5**. The differences may rise quite substantially, up to 54.3 kJ/mol in the case of the largest PAH (**5**) of this series taken into consideration in this work. The C−H bond strength corresponding to a hydrogen of a methyl group connected to a central ring is much smaller than a C−H bond involving a methyl group located near the border of the linear acene. The reason for this unexpected behavior must be traced back to geometrical features of the optimized reactants. Taking singly methylated anthracene (**3**) as a reference example, methylation at the central position (**3**-**9**) results in substantial repulsive effects between closely positioned hydrogen atoms, as shown schematically in Figure 5. The lower values of the BDEs must basically be traced back to a less stable character of the molecular compounds which are methylated in the middle compared to reactants with methylation at border positions (i.e., **3**-**9** compared to **3**-**1** and **3**-**2**). The steric hindrance at position **3**-**9** in the reactant lies at the origin of the apparently lower BDE of 345.8 kJ/mol compared with the BDE of 363.4 and 363.9 kJ/mol of **3**-**1** and **3**-**2**, respectively. To summarize, the 27 kJ/mol differences between the BDE values of **3**-**9** and toluene (**1**-**1**) can be traced back to a ±9 kJ/mol delocalization energy (calculated as the ΔBDE between **1**-**1** and **3**-**2**) and a ±18 kJ/mol steric hindrance (calculated as the ΔBDE between **3**-**2** and **3**-**9**). For the other compounds of the linear series, these values increase substantially. The differences between the BDE values of the four- and five-membered PAH on one hand and toluene on the other amount to 14 and 17 kJ/mol for the delocalization effect and 31 and 54 kJ/mol for the steric effect, respectively. The latter effect can furthermore be illustrated by calculating the BDE of the carbon−carbon bond between the attached methyl group and the aromatic substrate (vide supra). For nonlinear methylated PAHs (**6**−**16**), previous effects are overall not present. In this case, the structure models show a curled up geometry, and hence, extensive delocalization of the unpaired electron over the aromatic substrate is decreased. Due to the nonplanar geometry, the methyl group is naturally less hindered in the reactant complexes. For the majority of the species, the BDE approaches the reference value of toluene. Some deviations are noticed. This is mainly the case for species **10**-**14**, **11**-**16**, and **12**-**14**, where the local environment resembles anthracene-like substructures with methylation at the central position, and indeed, the corresponding C−H BDEs are very similar.

3.4. Influence of the Polyaromatic Environment on C−C BDEs. In addition to the previous results on C−H BDEs, we report on C−C BDE values, given in Table 4 and also depicted in Figure 4. Starting from the investigated set of methylated PAHs, the bond between the attached methyl group and the aromatic substrate is broken, resulting in the formation of arylic radicals. It is clearly seen that loss of a methyl hydrogen, forming a CH_2 group, is much easier than the breaking of an entire methyl group or loss of an aromatic hydrogen. It is also observed that the combination of steric effects and delocalization, encountered for the C−H BDEs in the linear series of benzylic radicals, is not present here. We are dealing with localized σ-type arylic radicals (also see ref 17). This can again be illustrated using methylated anthracene; the C−C BDE values of **3**-**9** and **3**-**2** correspond to 418.7 and 432.4 kJ/mol, respectively. The difference of 13.7 kJ/mol is again due to steric hindrance, as discussed before. A detailed analysis of the results of the nonlinear PAHs reveals large variations in the computed BDE values (a maximum range of 93 kJ/mol is reached). Similar to the C−H BDEs, the size of the polyaromatic is not determining. This is illustrated by comparing the results of **1**-**1** and **13**-**2**, which only deviate by 2 kJ/mol. The dominant effect is the local polyaromatic environment, defined by steric hindrance effects in the reactant structures and the planarity (linked to the degree of delocalization of the unpaired electron) of the product structures. For instance, comparison between the C−C BDE results of **7**-**1** and **7**-**2** amounts to 54 kJ/mol, with a reactant contribution (in absolute value) of 29 kJ/mol and a product contribution of 25 kJ/mol. It is moreover seen that the minimal C−C BDE values correspond to the structures **10**-**14**, **11**-**16**, and **12**-**14**, which are the most congested sites of the reactants, and consequently, detachment of the methyl group is highly preferred. To summarize, combining, in an appropriate way, all information on the homolytic cleavage of the C−H bond in PAHs and methylated PAHs leading to arylic and benzylic radicals, respectively, appears to succeed to reproduce correctly the observed reactivity trend for the C−C BDE values.

4. Conclusions

From the extensive set of calculations performed on potential reactive species during polyaromatic growth, we have deduced a number of important reactive characteristics based on carbon−hydrogen and carbon−carbon bond dissociation en-

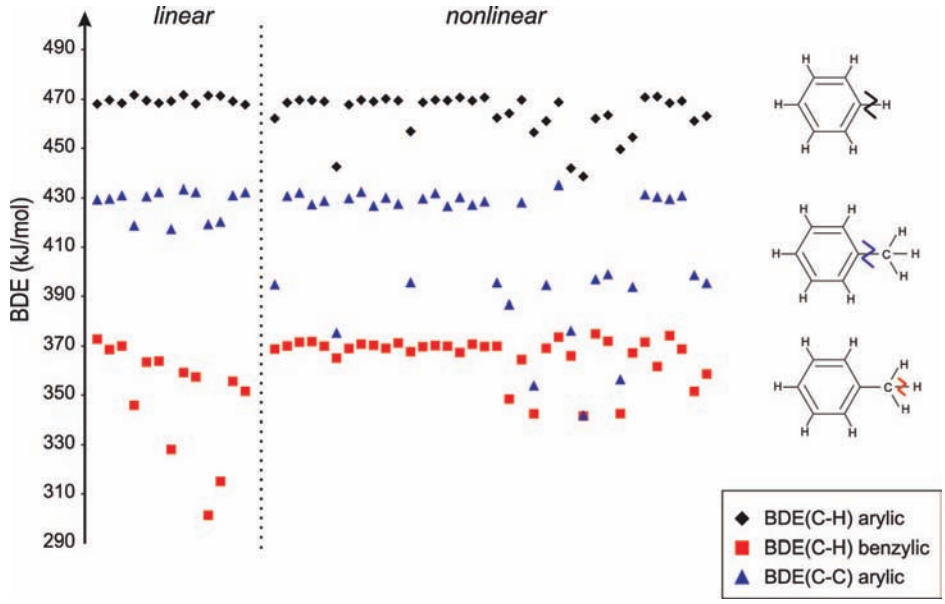

Figure 4. C−H and C−C BDEs (in kJ/mol) for the set of polyaromatics depicted in Figure 1. All values are calculated at BMK/6-311+G(3df,2p)//B3LYP/6-31+G(d,p).

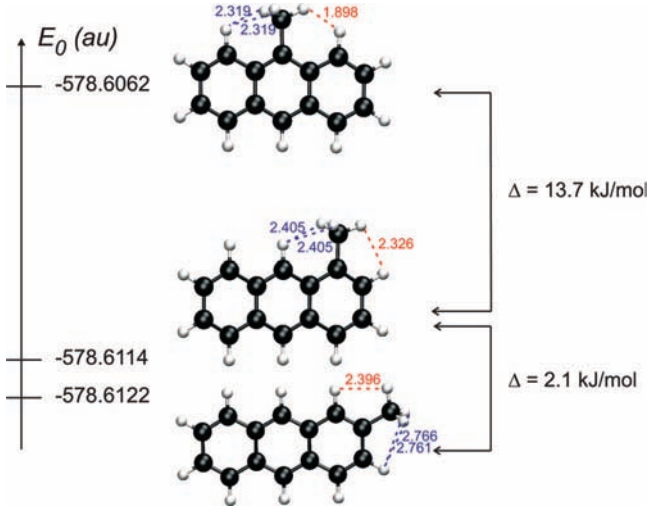

Figure 5. Optimized geometrical structures of **3-9**, **3-1**, and **3-2** obtained with B3LYP/6-31+G(d,p). Distances between adjacent hydrogens are given in Å. BMK//B3LYP energies (without ZPVEs) are also reported.

thalpies (BDEs). Three DFT functionals (i.e., B3P86, BMK, and M05-2X) were tested. A comparison with available experimental and computational data indicates the good performance of all functionals, with a slight preference for the B3P86 and BMK methods. For a selection of methylated PAHs, DFT results were assessed to benchmark G3(MP2)-RAD and SCS-ROMP2 in order to investigate the effect of delocalization of the unpaired electron and dispersion effects. The main factor contributing to the BDE value is the radical type that is considered. Arylic radicals are much more reactive for further reactions as they are less stable than benzylic radicals. However, benzylic radicals are more easily formed. The introduction of a polyaromatic environment induces for arylic radicals second-order effects on the BDEs, which must mainly be traced back to the stability of the parent molecule. Benzylic radicals originating from linear acenes show a distinct behavior due to two effects. Due to the π-character of the radical, they have the intrinsic potential to be stabilized by resonance effects. A second, less-expected effect is due to steric hindrance to which the methyl group is subjected in the parent molecule. If situated at central positions of linear acenes, steric hindrance is most pronounced, and creation of the radical induces relief of this strain. Both effects mentioned are not present for nonlinear methylated acenes as these reactants show a curled up geometry, which inhibits the mentioned features. Additional carbon−carbon BDEs (starting from methylated polyaromatics and leading to arylic radicals) are mainly determined by steric effects as also a σ-radical is formed which is not subject to delocalization. This study has once more shown the added value of theoretical calculations on systems for which no experimental data are available. Moreover, basic chemical insight is obtained from the quantitative numbers.

Acknowledgment. This work is supported by the Fund for Scientific Research-Flanders (FWO) and the Research Board of Ghent University.

References and Notes

(1) Luo, Y.-R. *Comprehensive Handbook of Chemical Bond Energies*; Taylor & Francis: Boca Raton, FL, 2007, and references therein.
(2) Blanksby, S. J.; Ellison, G. B. *Acc. Chem. Res.* **2003**, *36*, 255.
(3) DiLabio, G. A.; Pratt, D. A.; LoFaro, A. D.; Wright, J. S. *J. Phys. Chem. A* **1999**, *103*, 1653.
(4) Senosiain, J. P.; Han, J. P.; Musgrave, C. B.; Golden, D. M. *Faraday Disc.* **2001**, *119*, 173.
(5) Henry, D. J.; Parkinson, C. J.; Mayer, P. M.; Radom, L. *J. Phys. Chem. A* **2001**, *105*, 6750.
(6) Yao, X.-Q.; Hou, X.-J.; Jiao, H.-J.; Xiang, H.-W.; Li, Y.-W. *J. Phys. Chem. A* **2003**, *107*, 9991.
(7) Johnson, E. R.; Clarkin, O. J.; DiLabio, G. A. *J. Phys. Chem. A* **2003**, *107*, 9953.
(8) Coote, M. L.; Pross, A.; Radom, L. *Org. Lett.* **2003**, *5*, 4689.
(9) Feng, Y.; Liu, L.; Wang, J. T.; Huang, H.; Guo, Q. X. *J. Chem. Inf. Comput. Sci.* **2003**, *43*, 2005.
(10) Nam, P.-C.; Nguyen, M. T.; Chandra, A. K. *J. Phys. Chem. A* **2005**, *109*, 10342.
(11) Izgorodina, E. I.; Coote, M. L.; Radom, L. *J. Phys. Chem. A* **2005**, *109*, 7558.
(12) Zipse, H. *Top. Curr. Chem.* **2006**, *263*, 163.
(13) Izgorodina, E. I.; Brittain, D. R. B.; Hodgson, J. L.; Krenske, E. H.; Lin, C. Y.; Namazian, M.; Coote, M. L. *J. Phys. Chem. A* **2007**, *111*, 10754.
(14) Kaur, D.; Kaur, R. P.; Kaur, R. *J. Mol. Struct.: THEOCHEM* **2007**, *803*, 95.
(15) Menon, A. S.; Wood, G. P. F.; Moran, D.; Radom, L. *J. Phys. Chem. A* **2007**, *111*, 13638.
(16) Zhao, Y.; Truhlar, D. G. *J. Phys. Chem. A* **2008**, *112*, 1095.

(17) Van Speybroeck, V.; Marin, G. B.; Waroquier, M. *ChemPhysChem* **2006**, *7*, 2205.
(18) Wauters, S.; Marin, G. B. *Chem. Eng. J.* **2001**, *82*, 267.
(19) Hemelsoet, K.; Van Speybroeck, V.; Moran, D.; Marin, G. B.; Radom, L.; Waroquier, M. *J. Phys. Chem. A* **2006**, *110*, 13624.
(20) Van Speybroeck, V.; Hemelsoet, K.; Minner, B.; Marin, G. B.; Waroquier, M. *Mol. Simul.* **2007**, *33*, 879.
(21) Harvey, R. G. *Polycyclic Aromatic Hydrocarbons: Chemistry and Carcinogenicity*; Cambridge University Press: Cambridge, U.K., 1991.
(22) Denissenko, M. F.; Pao, A.; Tang, M. S.; Pfeifer, G. P. *Science* **1996**, *274*, 430.
(23) Allamandola, L. J. *Top. Curr. Chem.* **1990**, *153*, 1.
(24) *Polycyclic Aromatic Hydrocarbons and Astrophysics*; Léger, A., d'Hendecourt, L., Boccara, N., Eds.; NATO ASI Series C; Reidel;: Dordrecht, The Netherlands, 1987; Vol. 191.
(25) Yao, X.-Q.; Hou, X.-J.; Wu, G.-S.; Xu, Y.-Y.; Xiang, H.-W.; Jiao, H.-J.; Li, Y.-W. *J. Phys. Chem. A* **2002**, *106*, 7184.
(26) Zavitsas, A. A. *J. Phys. Chem. A* **2003**, *107*, 897.
(27) Bauschlicher, C. W.; Langhoff, S. R. *Mol. Phys.* **1999**, *96*, 471.
(28) Woodcock, H. L.; Schaefer, H. F., III; Schreiner, P. R. *J. Phys. Chem. A* **2002**, *106*, 11923.
(29) (a) Becke, A. D. *J. Chem. Phys.* **2003**, *119*, 2972. (b) Becke, A. D. *J. Chem. Phys.* **2005**, *122*, 064101. (c) Dickson, R. M.; Becke, A. D. *J. Chem. Phys.* **2005**, *123*, 111101.
(30) (a) Becke, A. D.; Johnson, E. R. *J. Chem. Phys.* **2007**, *127*, 124108. (b) Johnson, E. R.; Becke, A. D. *J. Chem. Phys.* **2008**, *128*, 124105.
(31) (a) Grimme, S. *J. Comput. Chem.* **2004**, *25*, 1463. (b) Schwabe, T.; Grimme, S. *Phys. Chem. Chem. Phys.* **2007**, *9*, 3397.
(32) (a) Grimme, S.; Diedrich, C.; Korth, M. *Angew. Chem., Int. Ed.* **2006**, *45*, 625. (b) Antony, J.; Grimme, S. *Phys. Chem. Chem. Phys.* **2008**, *10*, 2722.
(33) Frisch, M. J. Trucks, G. W.; Schlegel, H. B.; Scuseria, G. E.; Robb, M. A.; Cheeseman, J. R.; Montgomery, J. A., Jr.; Vreven, T.; Kudin, K. N.; Burant, J. C.; Millam, J. M.; Iyengar, S. S.; Tomasi, J.; Barone, V.; Mennucci, B.; Cossi, M.; Scalmani, G.; Rega, N.; Petersson, G. A.; Nakatsuji, H.; Hada, M.; Ehara, M.; Toyota, K.; Fukuda, R.; Hasegawa, J.; Ishida, M.; Nakajima, T.; Honda, Y.; Kitao, O.; Nakai, H.; Klene, M.; Li, X.; Knox, J. E.; Hratchian, H. P.; Cross, J. B.; Bakken, V.; Adamo, C.; Jaramillo, J.; Gomperts, R.; Stratmann, R. E.; Yazyev, O.; Austin, A. J.; Cammi, R.; Pomelli, C.; Ochterski, J. W.; Ayala, P. Y.; Morokuma, K.; Voth, G. A.; Salvador, P.; Dannenberg, J. J.; Zakrzewski, V. G.; Dapprich, S.; Daniels, A. D.; Strain, M. C.; Farkas, O.; Malick, D. K.; Rabuck, A. D.; Raghavachari, K.; Foresman, J. B.; Ortiz, J. V.; Cui, Q.; Baboul, A. G.; Clifford, S.; Cioslowski, J.; Stefanov, B. B.; Liu, G.; Liashenko, A.; Piskorz, P.; Komaromi, I.; Martin, R. L.; Fox, D. J.; Keith, T.; Al-Laham, M. A.; Peng, C. Y.; Nanayakkara, A.; Challacombe, M.; Gill, P. M. W.; Johnson, B.; Chen, W.; Wong, M. W.; Gonzalez, C.; Pople, J. A. *Gaussian 03*, revision D.01; Gaussian, Inc.: Wallingford, CT, 2004.
(34) Becke, A. D. *J. Chem. Phys.* **1993**, *98*, 5648.
(35) Lee, C.; Yang, W.; Parr, R. G. *Phys. Rev. B* **1988**, *37*, 785.
(36) Coote, M. L. *J. Phys. Chem. A* **2004**, *108*, 3865.
(37) Hemelsoet, K.; Moran, D.; Van Speybroeck, V.; Waroquier, M.; Radom, L. *J. Phys. Chem. A* **2006**, *110*, 8942.
(38) Boese, A. D.; Martin, J. M. L. *J. Chem. Phys.* **2004**, *121*, 3405.
(39) Vandeputte, A. G.; Sabbe, M. K.; Reyniers, M.-F.; Van Speybroeck, V.; Waroquier, M.; Marin, G. B. *J. Phys. Chem. A* **2007**, *111*, 11771.
(40) Zhao, Y.; Schultz, N. E.; Truhlar, D. G. *J. Chem. Theory Comput.* **2006**, *2*, 364.
(41) Grimme, S. *J. Chem. Phys.* **2003**, *118*, 9095.
(42) Jung, Y. S.; Lochan, R. C.; Dutoi, A. D.; Head-Gordon, M. *J. Chem. Phys.* **2004**, *121*, 9793.
(43) Henry, D. J.; Sullivan, M. B.; Radom, L. *J. Chem. Phys.* **2003**, *118*, 4849.
(44) Werner, H.-J.; Knowles, P. J.; Amos, R. D.; Bernhardsson, A.; Berning, A.; Celani, P.; Cooper, D. L.; Deegan, M. J. O.; Dobbyn, A. J.; Ecker, F.; Hampel, C.; Hetzer, G.; Knowles, P. J.; Korona, T.; Lindh, R.; Lloyd, A. W.; McNicholas, S. J.; Manby, F. R.; Meyer., W.; Mura, M. E.; Nicklass, A.; Palmieri, P.; Pitzer, R.; Rauhut, G.; Schutz, M.; Schumann, U.; Stoll, H.; Stone, A. J.; Tarroni, R.; Thorsteinsson, T.; MOLPRO 2002.6 University of Birmingham: Birmingham, U.K., 2002.
(45) Grimme, S. *J. Chem. Phys.* **2006**, *124*, 034108.
(46) Tsang, W. In *Energetics of Organic Free Radicals*; Simoes, J. A. M., Greenberg, A., Liebman, J. F., Eds.; Blackie Academie: NewYork, 1996.
(47) Berkowitz, J.; Ellison, G. B.; Gutman, D. *J. Phys. Chem.* **1994**, *98*, 2744.
(48) Fox, T.; Kollman, P. A. *J. Phys. Chem.* **1996**, *100*, 2950.
(49) McMillen, D. F.; Golden, D. M. *Annu. Rev. Phys. Chem.* **1982**, *33*, 493.
(50) Lias, S. G.; Bartmess, J. E.; Liebman, J. F.; Holmes, J. L.; Levin, R. D.; Mallard, W. G. *J. Phys. Chem. Ref. Data* **1988**, *17*, 1.
(51) Hrovat, D. A.; Borden, W. T. *J. Phys. Chem.* **1994**, *98*, 10460.
(52) Ellison, G. B.; Davico, G. E.; Bierbaum, V. M.; DePuy, C. H. *Int. J. Mass Spectrom. Ion Processes* **1996**, *156*, 109.
(53) Kasai, P. H.; Clark, P. A.; Whipple, E. B. *J. Am. Chem. Soc.* **1970**, *92*, 2640.
(54) Chen, R. H.; Kafafi, S. A.; Stein, S. E. *J. Am. Chem. Soc.* **1989**, *111*, 1418.
(55) Wang, H.; Frenklach, M. *J. Phys. Chem.* **1993**, *97*, 3867.
(56) Aihara, J.-I.; Fujiwara, K.; Harada, A.; Ichikawa, H.; Fukushima, K.; Hirota, F.; Ishida, T. *J. Mol. Struct.: THEOCHEM* **1996**, *366*, 219.
(57) Cioslowski, J.; Liu, G. H.; Martinov, M.; Piskorz, P.; Moncrieff, D. *J. Am. Chem. Soc.* **1996**, *118*, 5261.

JP801551C